Trans. JWRI, Vol. 22 (1993), No.1

Three Dimensional Numerical Simulation of Various Thermo-mechanical Processes by FEM (Report III)†

- Deformation Analysis of Compressors under Assembly by Plug Welding -

Yukio UEDA*, Jianhua WANG, Hidekazu MURAKAWA*** and Min Gang YUAN******

Abstract

Residual deformations and stresses after plug welding of a thin-wall cylinder with an inner bearing are analyzed. The numerical simulations are performed using the Thermal-Elastic-Plastic Finite Element Method. In these simulations 3-D solid element in which local coordinate system is introduced. In this element the reduced integration method is employed to prevent the numerical locking phenomena during bending deformation of the cylinder. The eccentricity of the bearing and the radial deformations at the end of the cylinder are analyzed for various cases with different conditions of plug welding. The computed results are compared with the measured values and good agreement is obtained. These simulations provide the possibility to predict the effects of various parameters on welding deformations and to control it to maintain high accuracy of the compressors. The residual stresses during plug welding are also calculated. The results show that the maximum principle stresses appear in the heat affected zone around the plug welds and reach high values.

KEY WORDS: (Plug Welding) (Compressor) (Eccentricity) (Residual Deformation) (Residual Stress) (Finite Element Method) (Locking Phenomena)

1. Introduction

The plug welding is used to assemble a thin-wall cylinder and an inner bearing of a compressor. Before this process, the cylinder is already assembled with a stator by shrinkage fit and with a housing by plug welding. The axis off the bearing may be deflected and its eccentricity may go beyond the allowable tolerance during the plug welding. On the other hand, the radial deformations are also caused especially at the ends of the cylinder. These may influence the following assembly processes to weld cap on the cylinder. In order to predict the welding deformations and to control the influential factors, the three dimensional numerical simulations using the Finite Element Method have been performed.

For 3-D thermal-elastic-plastic analysis by FEM, especially for the cases of high temperature such as welding problems, there are two main difficulties which should be considered. One is how to ensure the accuracy of computation and get the stable solution at the high temperature stages. The other is that it needs large memory capacity of computers and long CPU time. In order to solve realistic 3-D welding mechanical problems, fundamental studies on the following points have been conducted by the authors[1,2]:

(1) methods for improving the accuracy of 3-D heat conduction analysis by FEM and preventing or reducing the oscillation in temperature distribution due to the numerical error;
(2) methods for improving the accuracy and convergence of 3-D thermal-elastic-plastic analysis by FEM;
(3) coordinate transformation in 3-D models involving thin-wall cylinder;
(4) reduced integration method for preventing the locking phenomena, when the solid elements are used in the bending of a thin-wall cylinder;
(5) deformation analysis of compressors under assembly by shrinkage fit.

Based on the above researches, the welding deformations and stresses of a cylinder jointed with an inner bearing are simulated for various cases with different welding parameters. The eccentricities of the bearings and the radial deformations of the ends of the

† Received on August 2, 1993
* Professor
** Associate Professor, Shanghai Jiao Tong University
*** Associate Professor
**** Research Engineer, Daikin Industries, Ltd.

Transactions of JWRI is published by Welding Research Institute, Osaka University, Ibaraki, Osaka 567, Japan

cylinder are compared with the measured values obtained by experiments. The results show that good agreement can be obtained if the reduced integration method is applied to the cylinder. These simulations provide valuable informations which is very useful in controlling the accuracy in assembling a compressor. The residual stresses are also analyzed and it is found that the maximum principal stresses are observed in the HAZ around the plug welds and they reach very high values. Such information is very useful in discussing the probability of crack initiation.

2. Plug Welding of a Compressor and Its Modelling

2.1 Plug welding of a compressor

A thin-wall cylinder is jointed with an inner bearing by plug welding. Before this process the cylinder is already connected with a stator by shrinkage fit. Also it is joined with a housing by plug welding. **Figure 1** shows the diagram of a cylinder with the inner components. Then the ends of the cylinder will be assembled with spherical shells by circumferential welding in the following processes.

Three holes of 8 mm diameter are located with equal distance in the circumferential direction of the cylinder and plug welding by TIG welding are done simultaneously. The word "plug welding" means that the holes are filled with molten metal (plug) through the thickness of the cylinder, thus the inner part is connected with the cylinder by the welds.

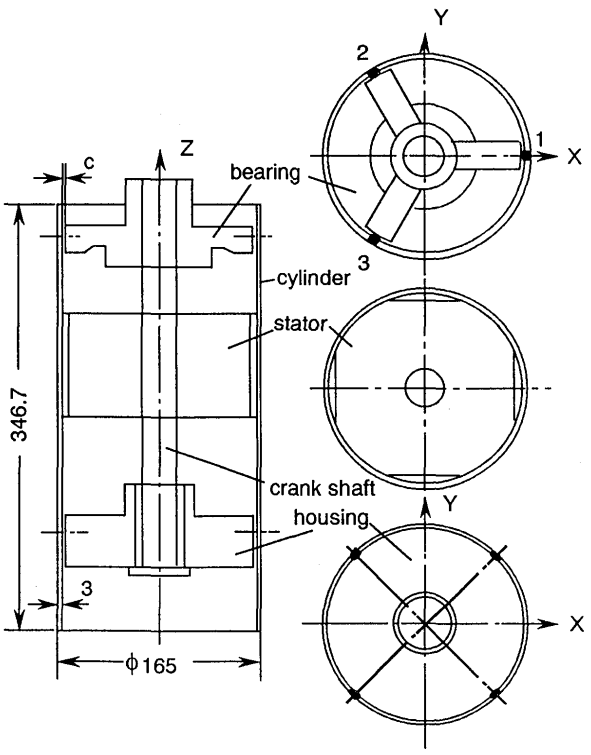

Fig.1 Diagram of a compressor.

2.2 Definition of eccentricity

After plug welding, the axis of bearing will move away from the ideal position due to the welding deformation. The eccentricity is defined based on the relative relation between the axes of bearing and that of the housing as shown in **Fig.2**. P_A is the intersection point of the axis of bearing with the base surface of the bearing, and P_B is the intersection point of the axis of bearing with the bottom surface of the housing. Distances A and B are the eccentricity of the bearing side and the housing side, respectively.

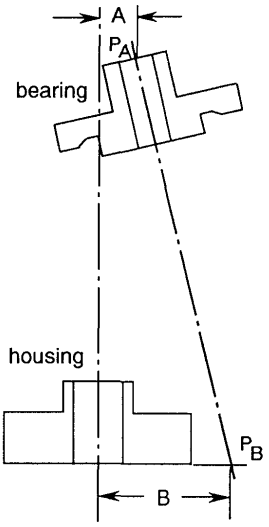

Fig.2 Definition of eccentricity.

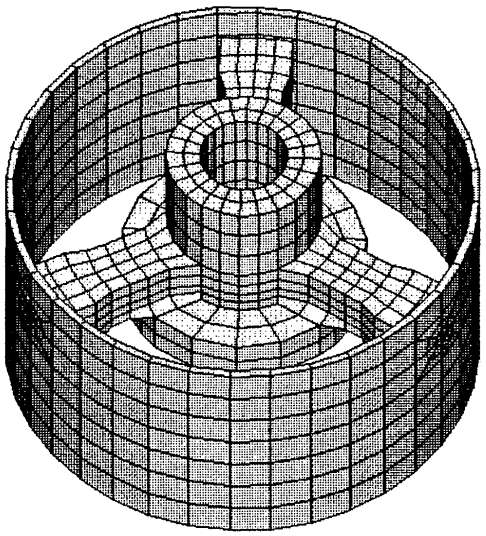

Fig.3 Simulation model.

2.3 Simulation models

In order to simplify the simulation model, a part of the cylinder containing only bearing is analyzed. The fixed boundary condition is used where the cylinder is in contact with the stator which has very large stiffness compared to the cylinder. The solid elements with the local coordinate system are used for the half of the structure. The mesh division is shown in **Fig.3**. The reduced integration method is applied to the cylinder to prevent the locking phenomena.

2.4 Material properties

The properties of material (SM41) and their temperature dependency used in the simulation are assumed based on experimental data and they are shown in **Fig.4**.

The thermal physical properties of the material are assumed as follows:

Heat conductivity

$$\lambda = (54.43-0.000042\cdot T^2)\cdot 10^{-3} \quad J/(mm\cdot s\cdot °C) \quad (1)$$

Thermal capacity

$$c = 0.41+0.00063\cdot T \quad J/(g\cdot °C) \quad (2)$$

Density

$$\rho = (7.82-2.625\cdot 0.001\cdot T)\cdot 10^{-3} \quad g/mm^3 \quad (3)$$

Heat transfer coefficient

$$\beta = 33.5\cdot 10^{-6} \quad J/(mm^2\cdot s\cdot °C) \quad (4)$$

Thermal expansion coefficient

$$\alpha = 1.3\cdot 10^{-5} \quad °C^{-1} \quad (5)$$

3. 3-D Heat Conduction Analysis by FEM

The discretized equation for 3-D heat conduction analysis by FEM can be written as follows,

$$(\theta[K]+[C]/\Delta t)\{T\}_n = ([C]/\Delta t-(1-\theta)[K])\{T\}_{n-1} + \theta\{Q\}_n+(1-\theta)\{Q\}_{n-1} \quad (6)$$

where, [K] = conductivity matrix;
[C] = thermal capacity matrix;
$\{Q\}_n$ = heat flow vector at present step;
$\{Q\}_{n-1}$ = heat flow vector at previous step;
$\{T\}_n$ = temperature at present step;
$\{T\}_{n-1}$ = temperature at previous step;
Δt = time increment;
θ = weight coefficient,
θ = 1/2: Crank-Nicolson method,
θ = 2/3: Galerkin method.

Because of the highly concentrated heat source which is applied on the weldment in a short time, so-called "oscillation phenomena" may be observed in the computed temperature field. In this paper, Galerkin method is used because the "oscillation phenomena" can be reduced compared with that using Crank-Nicolson method.

The heating processes include preheating before the welding stages. The electric current during welding is

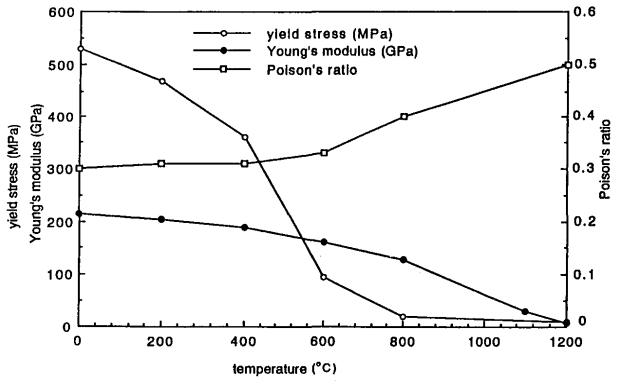

Fig.4 Temperature dependency of yield stress, Young's modulus and Poison's ratio.

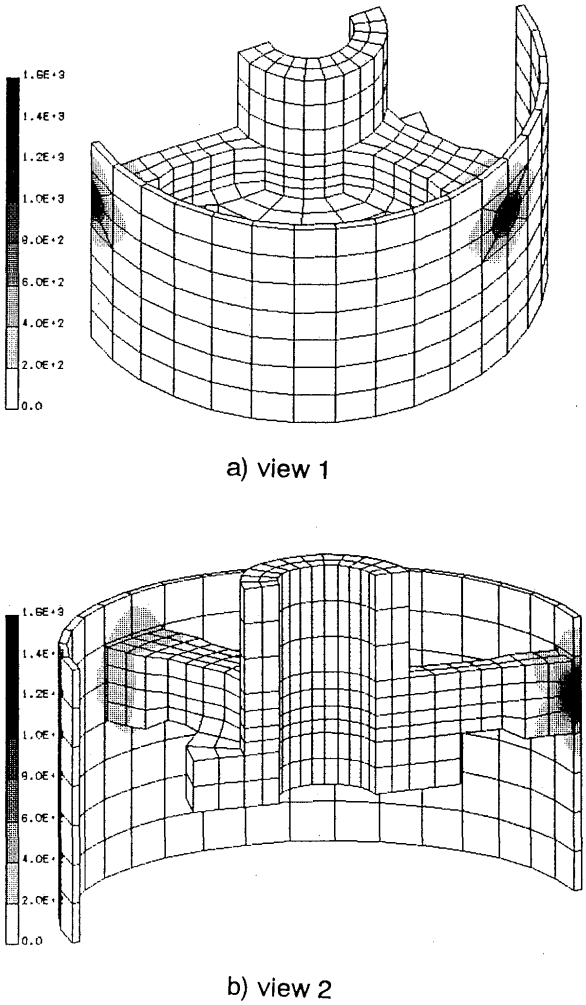

Fig.5 Temperature distributions at the end of heating process.

about 150-220 A and the total heating time is about 10-20 seconds. The heat of TIG welding is assumed to be applied uniformly to the volume of the hole to be filled with plug welding. The rates of heat input used for the present model are 10.5 J/(mm^3·s) and 21.0 J/(mm^3·s) during preheating stage and welding stage, respectively.

Figure 5 shows the temperature distributions of the model just at the end of the heating process. **Figures 6-a)** and **b)** show the thermal cycles at the points A and B on the surface of the cylinder which are 10 mm away from the center of the plug weld along horizontal and vertical directions respectively. These computed thermal cycles are compared with the measured ones in Fig. 6.

4. 3-D Thermal-Elastic-Plastic Analysis by FEM

4.1 Dummy elements

During preheating, there is no filled materials in the holes and the clearances between the cylinder and the bearing. To model these clearances, the dummy elements which has very small value of Young's modulus until the hole is completely filled are used.

4.2 Coordinate transformation

It is necessary to employ the cylindrical coordinates instead of rectangular Cartesian coordinates to analyze models with axisymmetrical geometry such as cylinders. In this case components of stresses and deformations can be decomposed into radial and circumferential directions. The use of local coordinate defined in the cylindrical coordinate makes it easy to introduce the reduced integration for particular components of the strain. The detail of the coordinate transformation has been presented in the previous report[2].

4.3 Locking phenomena and reduced integration method

The locking phenomena can be observed as the overestimation of stiffness[3], especially when the solid elements are used in the bending of a thin plate or a shell. In these cases, it would give the smaller deformations if the solid elements were not modified. Because the thickness of the cylinder considered in this study is thin, the locking phenomena may occur during the deformation due to the plug welds. In order to investigate the possibility of this phenomenon and its effects, two simplified models are considered as shown in **Figs. 7-a)** and **b)**. Model-a is a ring (d_1=150 mm, d_2=155.3 mm, b=10 mm) and model-b is a pipe (d=156.2 mm, t=3.2 mm, L=325 mm). Both are deformed by a pair of forces P.

Figure 8 shows the P-2f curves of model-a computed without and with reduced integration and they are compared with the analytical solution. The analytical solution of model-a is as follows,

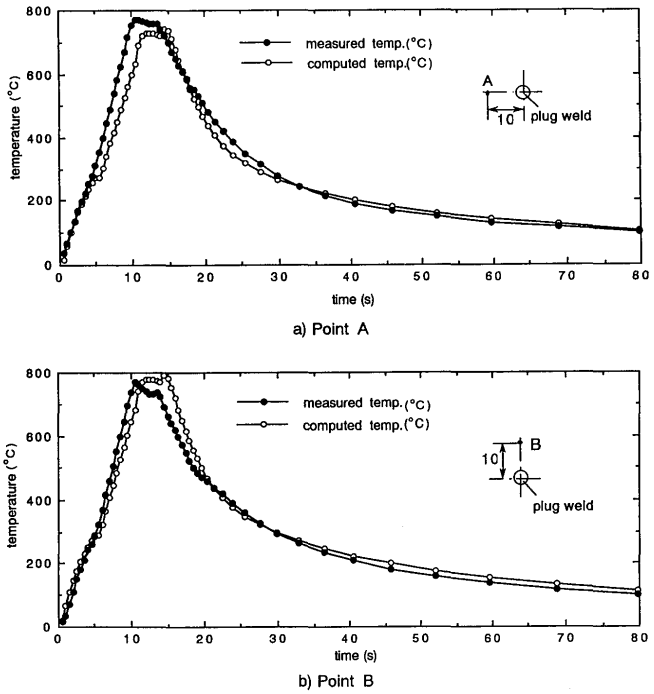

Fig.6 Heat cycles obtained by FEM and experiments.

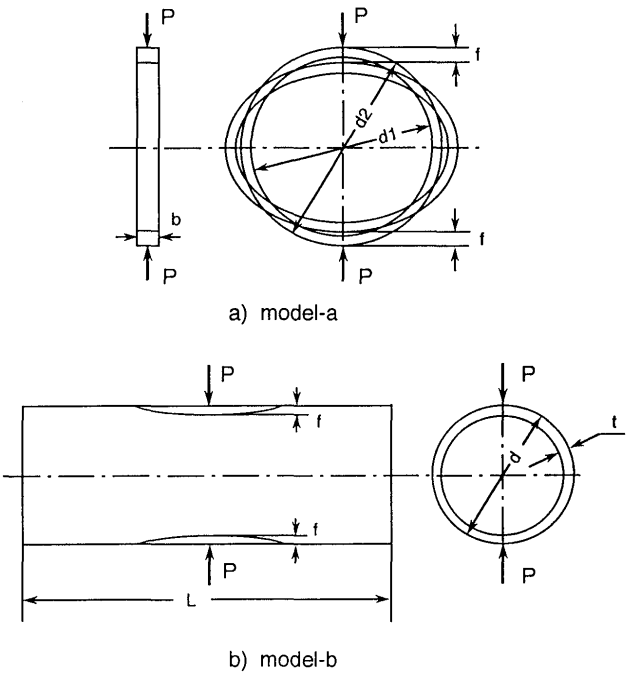

Fig.7 Simplified models for checking locking phenomena.

$$2f = Pr^3(\frac{\pi}{4} - \frac{2}{\pi}) / EJ \quad (7)$$

where, 2f = total displacement in loading direction;
r = average radius of the ring;
E = Young's modulus;
J = moment of inertia of the cross-section.

Figure 9 shows the calculated results of P-2f curves of model-b under the conditions of without and with reduced integration. From Figs.8 and 9, it can be seen that the locking phenomena has a significant effect in both models when the solid elements are used without reduced integration. The use of reduced integration can prevent the locking and give closer value to the analytical solution.

4.4 A accuracy and convergence of computation

The factors which influence the accuracy of the computation and convergence of 3-D thermal-elastic-plastic analysis have been investigated and some methods to improve the accuracy are proposed[1]. According to the computed results obtained in this study. The computed accuracy changes with the stages in the welding process. **Table 1** shows the error involved in the approximate solution at the given step after five iterations. The error is defined as following equation,

$$Err = \frac{\sqrt{\Sigma F_i^2}}{\sqrt{\Sigma F_j^2}} \quad (8)$$

where, F_i = the force at the free node i produced as error;
F_j = the reaction force at the fixed node j.

The convergence can be reached after iterations in all computation stages shown Table 1. However, big number of iteration are required when the temperature is high. To reduce iteration, further improvement of the computation scheme is necessary.

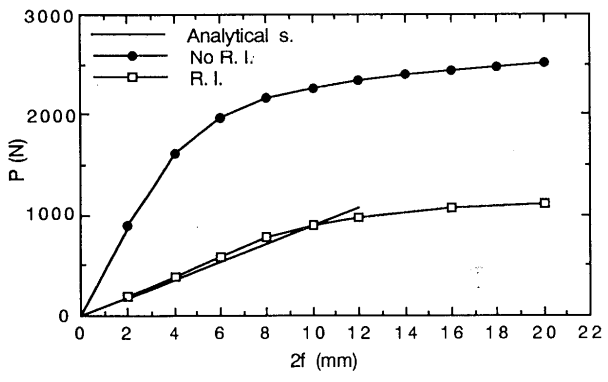

Fig.8 Load-displacement curves of model-a.

5. Simulation Results and Discussions

5.1 Influential factors for welding deformations

The following factors are examined as the potential cause of eccentricity:

(1) variation of heat input during TIG welding;
(2) unsymmetry caused by the combination of bearing (rotational symmetry with 120°) and stator (rotational symmetry with 90°);
(3) differences of clearances between the cylinder and the bearing before welding;
(4) time lag among the three plug weldings;
(5) deviations of the locations of plug welds;
(6) influence of the fixtures.

5.2 Eccentricities

Table 2 shows the eccentricities of the bearing after plug welding under the different conditions. The definition of eccentricity A and B can be found in Fig.2. As Fig.1 shows, the stator and the housing are joined to the cylinder with shrinkage fit and plug weldings, respectively, prior to the welding of the bearing. The stator has the rotational symmetry with 90° and the bearing has that of 120°. The combination of these two introduces asymmetry and it may cause the eccentricity. Thus the effect of the shape of the stator is examined by using two different boundary conditions at the lower end of the model shown by Fig.3. In one model, the stator is assumed to have the complete circular shape and all point at the lower end are fixed. In the other model, the nodes locate at the gap is left free. The former boundary

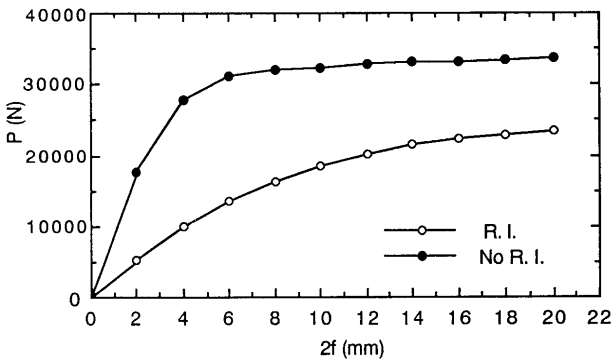

Fig.9 Load-displacement curves of model-b.

Table 1 A accuracy of computation in the different stage.

Stages	Err
Elastic	$<10^{-12}$
El-Pl (<500℃)	10^{-5}-10^{-7}
El-Pl (500-800℃, usually)	10^{-4}-10^{-6}
El-Pl (500-800℃, specilly)	10^{-2}-10^{-3}

condition is refereed to as uniform and the latter as ununiform in Table 2. In Table 2, c_1, c_2 and c_3 are the clearances at the points of plug welds 1, 2 and 3, respectively as shown in Fig.1. Δt is the difference between the starting time of TIG welding of plug welds of 1 and that of 2 and 3. Δh is the coordinate deviation of the position in z direction between plug welds 1 and the other two.

From Table 2 it can be seen that the eccentricities are caused seriously by the difference in clearances, time lag in welding and deviations of the locations of plug welds. The eccentricity can be reduced by using the fixtures such as chuck and clamp during welding. However the effects of fixture depend on the position to be fixed and it should be selected carefully. The eccentricities in the real compressor due to plug welding appear as a result of a combination of all the factors mentioned above.

The experimental results of eccentricity varies depending on the test conditions. However it is about in the limits of ±0.08 mm when the clearances between the cylinder and bearing are in the range of 0.35-0.6 mm. The calculated results are found to agree well with the experimental values in tendency. The advantages of the simulation is the possibility to examine the effects of individual factors in detail and the information can be utilized to reduce the deformations by controlling the influential factors.

Table 2 Welding deformations under different conditions.

No	Conditions of plug welding						Welding deformations			
	boundry c.	c_1	c_2=c_3	Δt	Δh	fixture	A	B	ΔR_1	ΔR_2
1	uniform	0.45	0.45	0	0	---	0	0	0.294	0.294
2	ununiform	0.45	0.45	0	0	---	-0.002	0.005	0.294	0.295
3	••	1.00	0.20	0	0	---	-0.050	-0.058	0.333	0.304
4	••	0.20	1.00	0	0	---	0.042	0.065	0.297	0.330
5	••	0.45	0.45	+3	0	---	-0.032	-0.024	0.290	0.293
6	••	0.45	0.45	-3	0	---	0.027	0.033	0.295	0.293
7	••	0.45	0.45	0	+3	---	-0.007	0.042	0.327	0.293
8	••	0.45	0.45	0	-3	---	0.001	-0.030	0.234	0.289
9	••	1.00	0.20	0	0	R**	0.005	-0.025	0.333	0.305
10	••	1.00	0.20	0	0	R, Z**	0.010	-0.058	0.333	0.302
11	••	0.45	0.45	*	0	---	0.155	-1.433	0.199	--
12	••	0.45	0.45	*	0	R, Z	0.215	-1.990	0.196	--

* only point 1 is welded.

** R and Z: bearing is fixed in radial and axis direction respectively.

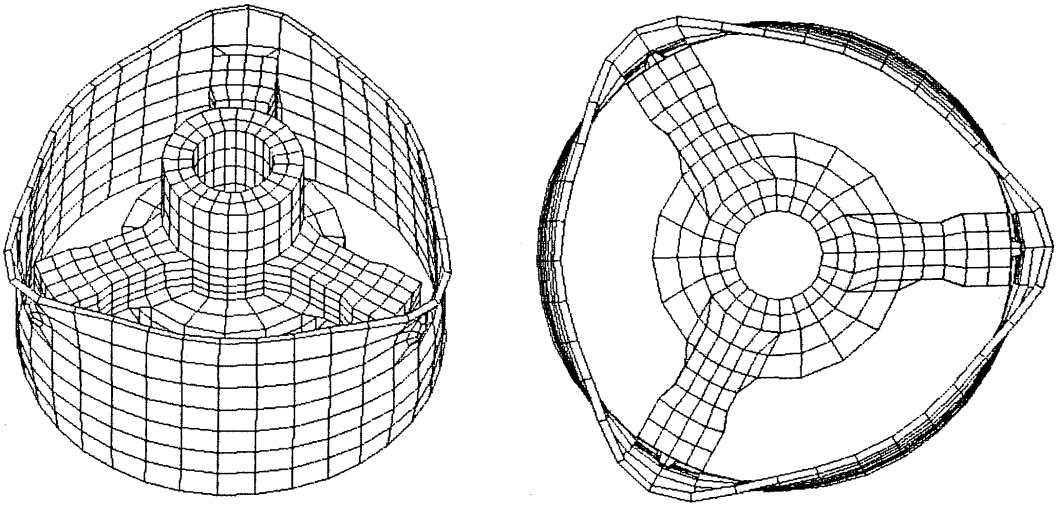

a) view 1 b) view 2

Fig.10 Residual deformations.

5.3 "Flower pattern" deformation

Figures 10-a) and **b)** show the residual deformations of the model after plug welding. The shape of the radial deformation at the end of the cylinder looks like a "flower pattern". **Figure 11** shows the comparison between the computed and measured deformations. The values of radial expansion on the top end of the cylinder just above the plug welds 1 and 2 (ΔR_1 and ΔR_2) are also shown in Table 2, and they are very close to the measured data (0.3-0.4 mm). Such deformations may influence the following assembly process, which is the circumferential welding of spherical shells onto the ends of the cylinder.

5.4 Characteristic of residual stresses

Figure 12 shows the distributions of residual stresses of the model. The largest component of the principal stress is shown in this figure. It is interesting to notice that the maximum stresses are observed in HAZ around the plug welds and it reaches the yield stress.

6. Conclusions

(1) The welding deformations and stresses of a compressor have been simulated successfully by 3-D thermal-elastic-plastic analysis. The solid elements with reduced integration scheme and local coordinate system are used for preventing the locking phenomena. The accuracy of computation and and convergence can be achieved in all the computation stages during welding. The calculated results are found to agree well with the experimental values.

(2) The influence of the following factors on the eccentricity are examined,

a. heat input of TIG welding;
b. clearances between the cylinder and bearing;
c. time lag among the three plug weldings;
d. deviation in the position of welds;
e. use of the fixtures.

The precision in assembling compressors by plug welding can be maintained by controlling the above parameters according to the information obtained by the 3-D numerical simulations as shown in Table 2.

(3) The "flower pattern" deformations at the end of the cylinder are simulated. The calculated shapes are very close to the measured curves. The computed values of the radial expansion of the cylinder are almost the same as the experiment.

(4) The distributions of residual stresses are also analyzed. The maximum principle stresses are observed in HAZ around the plug welds and they reaches the yield stress.

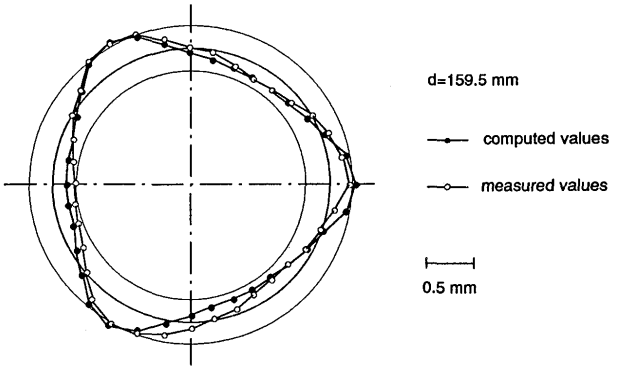

Fig.11 "Flower pattern" deformations.

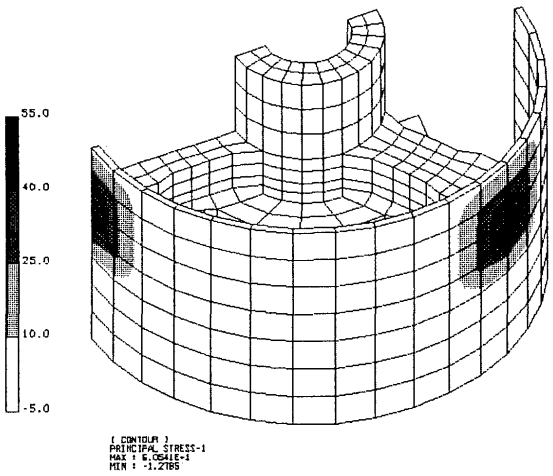

a) view 1

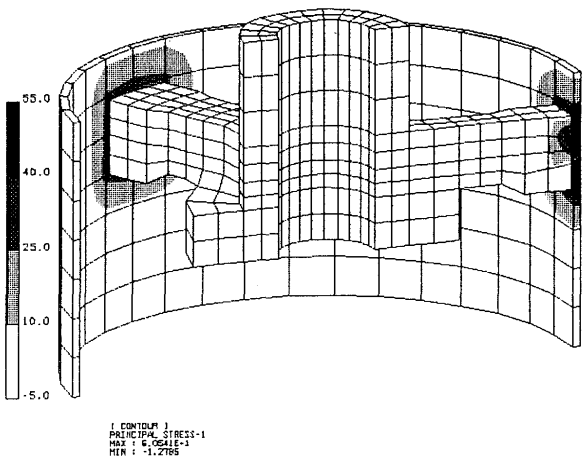

b) view 2

Fig.12 Distributions of residual stresses.

References

1) Y. Ueda et. al., "Three Dimensional Numerical Simulation of Various Thermal-mechanical Processes by FEM (Report I) Methods for Improving the Convergence of 3-D Analysis of Welding", Trans. JWRI, Vol.21, No.2, 1992, pp.111-117.

2) Y. Ueda et. al., "Three Dimensional Numerical Simulation of Various Thermal-mechanical Processes by FEM (Report II) Deformation Analysis of Compressors under Assembly by Shrinkage Fit",Trans. JWRI, Vol.21, No.2, 1992, pp.119-124.

3) N. Carpenter et. al., "Locking and Shear Scaling Factors in C^0 Bending Elements", Computers & Structures, Vol.22, No.1, 1986, pp.39-52.